

CHANDRA LOCALIZATION OF XTE J1906+090 AND DISCOVERY OF ITS OPTICAL AND INFRARED COUNTERPARTSERSIN GÖĞÜŞ,^{1,2} SANDEEP K. PATEL,^{2,3} COLLEEN A. WILSON,^{3,4} PETER M. WOODS,^{2,3}
MARK H. FINGER,^{2,3} AND CHRYSsa KOUVELIOTOU^{3,4}

Received 2005 May 15; accepted 2005 June 28

ABSTRACT

We present the *Chandra* identification and localization of the transient X-ray source XTE J1906+090 and the discovery of its optical and infrared counterparts. Our analysis of archival *Chandra* ACIS-I observations of the field found the source approximately $8'$ away from the position determined earlier with the *RXTE* PCA. We have confirmed the source identification with timing analysis of the X-ray data, which detected the source spin period of 89.6 s. The best *Chandra* position for the source is R.A. = $19^{\text{h}}04^{\text{m}}47^{\text{s}}.491$, decl. = $+09^{\circ}02'41''.40$. Subsequently, we performed optical observations of the field around the new location and discovered a coincident optical source with R -band magnitude of 18.7. A search in the Two Micron All Sky Survey catalog revealed an infrared point source with $J = 15.2$, $H = 14.2$, and $K = 13.5$, whose location is also coincident with our *Chandra* and optical positions. Our results add fresh evidence for a Be/X-ray transient nature for XTE J1906+090.

Subject headings: infrared: stars — pulsars: individual (XTE J1906+090) — X-rays: binaries

1. INTRODUCTION

XTE J1906+090 is a transient X-ray pulsar with a period of $P = 89$ s. It was discovered during an outburst with the *Rossi X-Ray Timing Explorer* Proportional Counter Array (*RXTE* PCA) in 1996 September (Marsden et al. 1998). The source was detected in outburst again in 1998 September. The *RXTE* PCA scanning observations of the field during the latter epoch localized XTE J1906+090 at R.A. = $19^{\text{h}}05^{\text{m}}20^{\text{s}}$, decl. = $+09^{\circ}02'30''$ with an estimated error of $2'$ at the 90% confidence level (Takeshima & Murakami 1998). This transient is below the detection threshold of the All Sky Monitor (ASM) on board *RXTE*; thus, little is known about its long-term flux history.

Wilson et al. (2002) performed the most extensive spectral and temporal investigations of both XTE J1906+090 outbursts to date. The source flux (2–10 keV) in 1996 and 1998 was measured to be 6.0×10^{-12} and 1.1×10^{-10} ergs $\text{cm}^{-2} \text{s}^{-1}$, respectively. During the brighter 1998 outburst, there is a detection of an iron line whose flux positively correlates with the 2–30 keV pulsed flux. A spin frequency of 0.01121178(1) Hz and short-term frequency rate of -4×10^{-12} Hz s^{-1} were measured during the 30 day long outburst in 1998 September (Wilson et al. 2002). Based on the spectral and temporal characteristics of the source during both activity intervals, it was suggested that XTE J1906+090 is in a Be/X-ray binary system (Marsden et al. 1998; Wilson et al. 2002).

Be/X-ray stellar binary systems consist of an accreting neutron star in an eccentric orbit with a Be star: a spectral B-type star that displays Balmer emission lines in its optical spectrum (Coe 2000). Be/X-ray binaries often undergo X-ray outburst cycles. These outbursts are typically classified into two categories: (1) normal outbursts with luminosities around 10^{35} – 10^{37} ergs s^{-1} , lasting for a few days or weeks and generally coincident with the time of the periastron passage of the neutron

star and (2) giant outbursts with luminosities $\geq 10^{38}$ ergs s^{-1} and lasting for weeks or months (Stella et al. 1986; Negueruela 1998).

Be stars are also strong infrared (IR) light emitters. Both the Balmer emission lines and the IR radiation are thought to originate from the circumstellar disk of material around the star. Another distinguishing property of Be stars is their high rotation rates, which can reach up to $\sim 70\%$ of the critical breakup velocity. These excessive rotation rates are thought to play a role in the formation of a circumstellar disk (Porter & Rivinius 2003).

In this paper, we report the X-ray identification of XTE J1906+090 in archival *Chandra* observations and our subsequent optical observations of the source with the Russian-Turkish Telescope (RTT150), which resulted in the discovery of its counterpart. In §§ 2 and 3, we describe our observations and data analyses. We discuss the implications of our results in § 4 and summarize our conclusions in § 5.

2. X-RAY OBSERVATIONS

XTE J1906+090 was observed with the *Chandra X-Ray Observatory* (Weisskopf 2004) Advanced CCD Imaging Spectrometer-Imaging Array (ACIS-I; Garmire et al. 2003) for 13.4 ks on 2003 May 26 (MJD 52,785; ObsID 3793) to obtain a precise localization of the source. The aim point of the ACIS-I array was set to the position obtained earlier with the PCA scanning observations (Takeshima & Murakami 1998).

We processed the data using the `acis_process_events` tool of the *Chandra* Interactive Analysis of Observations (CIAO,⁵ ver. 3.2.1) to reproduce the level 2 event list and removed the pixel randomization. For the calibration we used the *Chandra* CALDB,⁶ version 3.0.1.

2.1. Source Location

To identify X-ray sources in the ACIS-I field ($16'.9 \times 16'.9$), we generated a binned (by a factor of 2) and energy-filtered

¹ Faculty of Engineering and Nuclear Science, Sabanci University, Orhanlı-Tuzla, İstanbul 34956, Turkey; ersing@sabanciuniv.edu.

² Universities Space Research Association, 7501 Forbes Boulevard, Suite 206, Seabrook, MD 20706.

³ XD-12, Space Science Branch, National Space Science and Technology Center, 320 Sparkman Drive, Huntsville, AL 35805.

⁴ NASA Marshall Space Flight Center.

⁵ See <http://cxc.harvard.edu/ciao>.

⁶ See <http://cxc.harvard.edu/caldb>.

TABLE 1
X-RAY POINT SOURCES IN THE *Chandra* ACIS-I FIELD OF XTE J1906+090

| Source Number | R.A. (J2000.0) | Decl. (J2000.0) | 1 σ Error (arcsec) | Off-Axis Distance (arcmin) | Net Counts | S/N |
|---------------|-------------------|--------------------|------------------------------|-------------------------------|------------|------|
| 1..... | 19 05 21.42 | +09 09 21.2 | 0.72 | 6.60 | 16 | 3.6 |
| 2..... | 19 05 28.72 | +09 14 56.0 | 1.98 | 12.36 | 17 | 3.4 |
| 3..... | 19 05 29.55 | +09 06 19.3 | 0.49 | 4.30 | 13 | 3.2 |
| 4..... | 19 05 32.98 | +09 13 09.1 | 1.91 | 10.88 | 12 | 2.9 |
| 5..... | 19 05 40.10 | +09 04 00.8 | 0.47 | 5.17 | 29 | 4.7 |
| 6..... | 19 05 43.42 | +08 57 26.8 | 0.63 | 7.90 | 27 | 4.7 |
| 7..... | 19 05 46.90 | +08 59 31.2 | 0.52 | 7.45 | 56 | 6.5 |
| 8..... | 19 04 47.49 | +09 02 41.4 | 0.33 | 7.97 | 961 | 27.4 |
| 9..... | 19 04 55.38 | +08 59 54.2 | 0.48 | 6.67 | 56 | 6.6 |
| 10..... | 19 04 59.20 | +09 00 26.7 | 0.55 | 5.59 | 16 | 3.7 |
| 11..... | 19 05 07.66 | +08 54 34.4 | 1.08 | 8.73 | 17 | 3.6 |
| 12..... | 19 05 15.19 | +08 59 51.2 | 0.43 | 3.13 | 13 | 3.1 |

NOTE.—Units of right ascension are hours, minutes, and seconds, and units of declination are degrees, arcminutes, and arcseconds.

(0.5–8.0 keV) image of the entire ACIS-I field. We used the source detection method described in § 3.1 of Swartz et al. (2003) with a signal-to-noise (S/N) ratio of 2.8 and a minimum 5σ above background as our detection threshold; this corresponds to a background-subtracted point-source detection limit of 12 counts. The resulting source positions (J2000.0), approximate positional errors (68% confidence level), count rates, and S/Ns are listed in Table 1.

The circle near the center of the ACIS-I array in Figure 1 indicates the $2'$ error circle centered at the PCA position. We found no sources within this error circle with a 3σ flux upper limit of 1.2×10^{-15} ergs cm $^{-2}$ s $^{-1}$ (0.5–10.0 keV). There is, however, a point X-ray source (about $8'$ away from the PCA position, encircled in the upper right ACIS-I chip in Fig. 1; see also source No. 8 in Table 1) that was bright enough to allow for detailed timing and spectral analyses. Timing analysis of CXO

J190447+090241 revealed 89.6 s pulsations, thus confirming that it is XTE J1906+090, as we show in § 2.2. We note that large inaccuracies in a source position as determined with the PCA scanning observations can occur, especially when the source intensity varies on timescales of order the timescale of the scans, the source is located close to the Galactic ridge, the source is weak, or there are other bright X-ray sources within a few degrees of the object of interest. All four factors were present during the *RXTE* scan of XTE J1906+090.

As Table 1 shows, source 8 is by far the brightest in the field. To further improve the precision of its X-ray position, we applied the following method. We extracted an image with a $15''$ radius about the source and fitted the image using a two-dimensional elliptical Gaussian model to derive a best-fit centroid. The shape parameters of the source are $\sigma_1 = 2''.11$ ($\pm 0''.07$) and $\sigma_2 = 0''.88$ ($\pm 0''.03$), and a position angle of $65^\circ 8' \pm 1''.2$, which are consistent with the point-spread function (PSF) for a source at this off-axis location. The statistical errors in the source centroid are $0''.03$ in right ascension and $0''.05$ in declination. To check for any offset between the derived Gaussian centroid and the true source location, we have simulated a source at the same off-axis location and with the same source spectrum using the *Chandra* simulation tools ChaRT⁷ and MARX.⁸ We then compared the input position to the position derived from a fit to the simulated data and found a negligible offset of $< 0''.04$ in both right ascension and declination. We determine that the best-fit *Chandra* location for XTE J1906+090 is R.A. = $19^{\text{h}}04^{\text{m}}47^{\text{s}}.491$, decl. = $+09^\circ 02' 41''.40$. The error radius is determined by adding in quadrature the *Chandra* aspect uncertainty of $0''.6$ and the uncertainty in the derived source position of about $0''.17$, which results in $0''.62$ (at the 90% confidence level).

2.2. Timing Analysis

To unambiguously identify CXO J190447+090241, described in the previous section as XTE J1906+090, we performed a timing analysis in the *Chandra* data, as follows. We extracted all X-ray counts from a $15''$ circular region centered at the source position and converted their arrival times to the solar system barycenter. We employed the Z_m^2 statistic to search for a periodic signal in the data (Buccheri et al. 1983), focusing in the

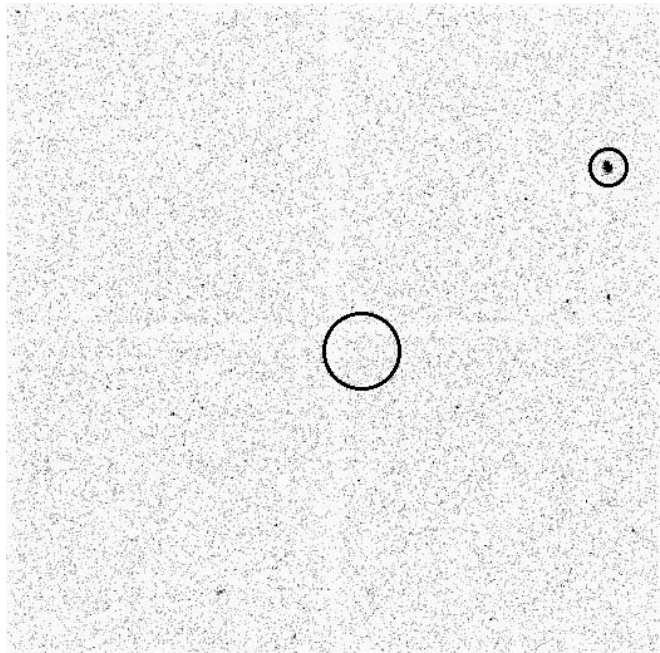


FIG. 1.—*Chandra* ACIS-I X-ray image of the vicinity of XTE J1906+090. The $2'$ radius circle near the center indicates the position obtained with the *RXTE* PCA scanning observations. The point source on the upper right side (encircled by an illustrative $2'$ radius circle) is XTE J1906+090.

⁷ See <http://asc.harvard.edu/chart>.

⁸ See <http://space.mit.edu/CXC/MARX>.

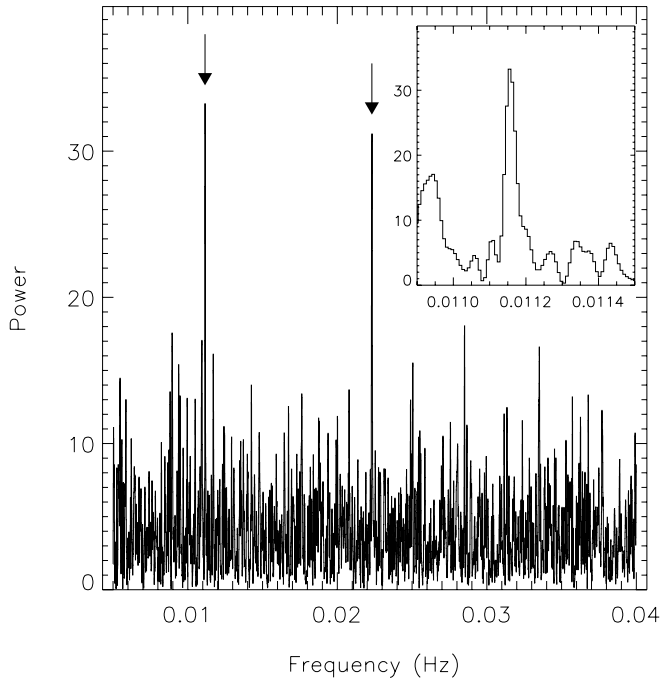


FIG. 2.—Plot of the Z_2^2 power spectrum of XTE J1906+090 derived from the *Chandra* ACIS-I observation of the source. The left (right) arrow indicates the coherent pulsations at the fundamental (first harmonic) spin frequency. The inset shows a periodicity search in a narrow frequency range (see text).

frequency range of 0.005–0.04 Hz. First we used the Z_1^2 statistic and detected a strong signal at 0.022308 Hz, which is nearly twice the spin frequency of XTE J1906+090 as measured in 1998 (Wilson et al. 2002). Motivated by this detection, we further searched the data with the Z_2^2 statistic. The latter search yielded the detection of the fundamental spin frequency at 0.011153 ± 0.000003 Hz. In Figure 2, we show the Z_2^2 power spectrum. The corresponding spin period is 89.66 ± 0.03 s, in good agreement with the value found by Wilson et al. (2002), which clearly indicates that CXO J190447+090241 is XTE J1906+090.

We performed a Monte Carlo simulation to determine the significance of the periodicity. For this we generated 10^6 simulated data sets, each containing 961 total source photons randomly distributed over a 13.4 ks interval, and then performed a Z_2^2 periodicity search on each data set. These searches were limited to the frequency range of 0.0109–0.0115 Hz (see the inset in Fig. 2), which was obtained by assuming that the average spin-up (or -down) from the spin frequency of 0.011212 Hz was less than the $|\dot{\nu}|$ of 4×10^{-12} Hz s $^{-1}$ measured in the 1998 outburst (Wilson et al. 2002). Out of 10^6 simulated data sets, we found that only 41 cases resulted in Z_2^2 power values exceeding that of the peak value of 33.4 in Figure 2. We find the chance coincidence probability of the detected signal is 4.1×10^{-5} .

Figure 3 shows two cycles of the pulse profile of XTE J1906+090 in the energy range of 1.0–8.0 keV. We calculate the rms pulse fraction as 0.21 ± 0.03 . Comparison of this profile with the 2–10 keV pulse profiles observed during the 1996 and 1998 outbursts (Wilson et al. 2002) indicates significant changes in the pulse shape. In particular, the 2003 pulse profile more closely resembles the 1996 shape than the one observed in 1998.

Finally, we note that the light curve of XTE J1906+090 shows significant intensity variations on timescales longer than the spin period of the system (see Fig. 4). A power spectral

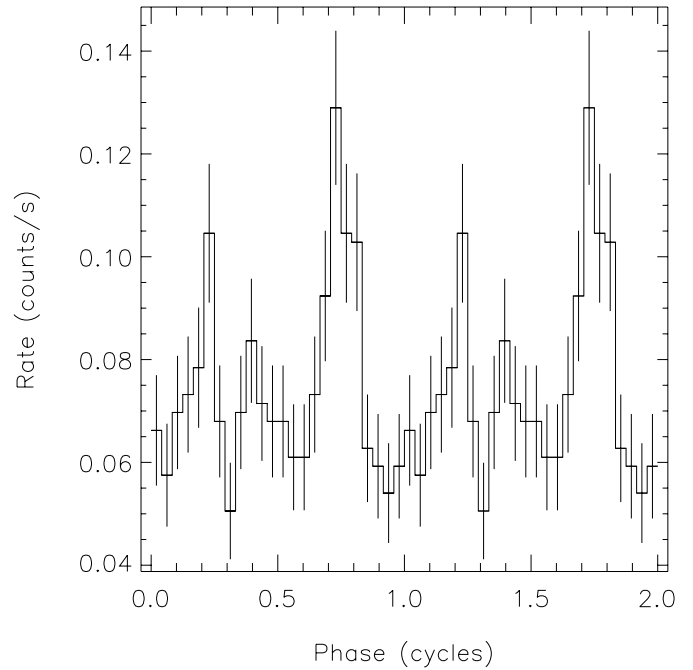


FIG. 3.—*Chandra* pulse profile of XTE J1906+090 derived in the 1.0–8.0 keV energy range.

analysis showed low-frequency noise with an rms fractional amplitude of $34\% \pm 7\%$ between 7×10^{-5} and 2.5×10^{-3} Hz. Above 5×10^{-3} Hz there was no evidence for source variability other than the pulsations from XTE J1906+090.

To check whether low-frequency variations persist in XTE J1906+090, we investigated seven *RXTE* pointings that took place around the peak of the 1998 outburst epoch. We found evidence for low-frequency noise with an rms fractional amplitude of 10%–28%. However, because *RXTE* is not an imaging instrument, we cannot definitively say whether this noise was

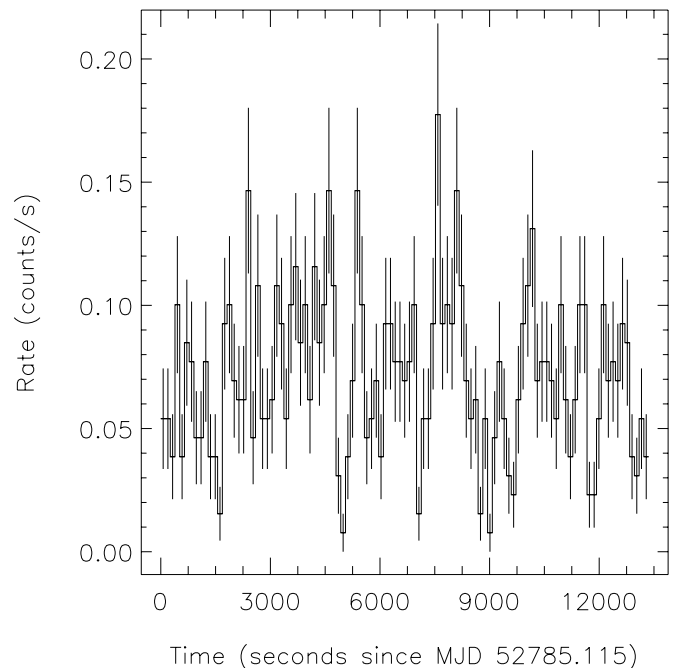


FIG. 4.—Background-subtracted X-ray light curve of XTE J1906+090 (in 1.0–8.0 keV) in 128 s time bins. The error bars indicate statistical errors.

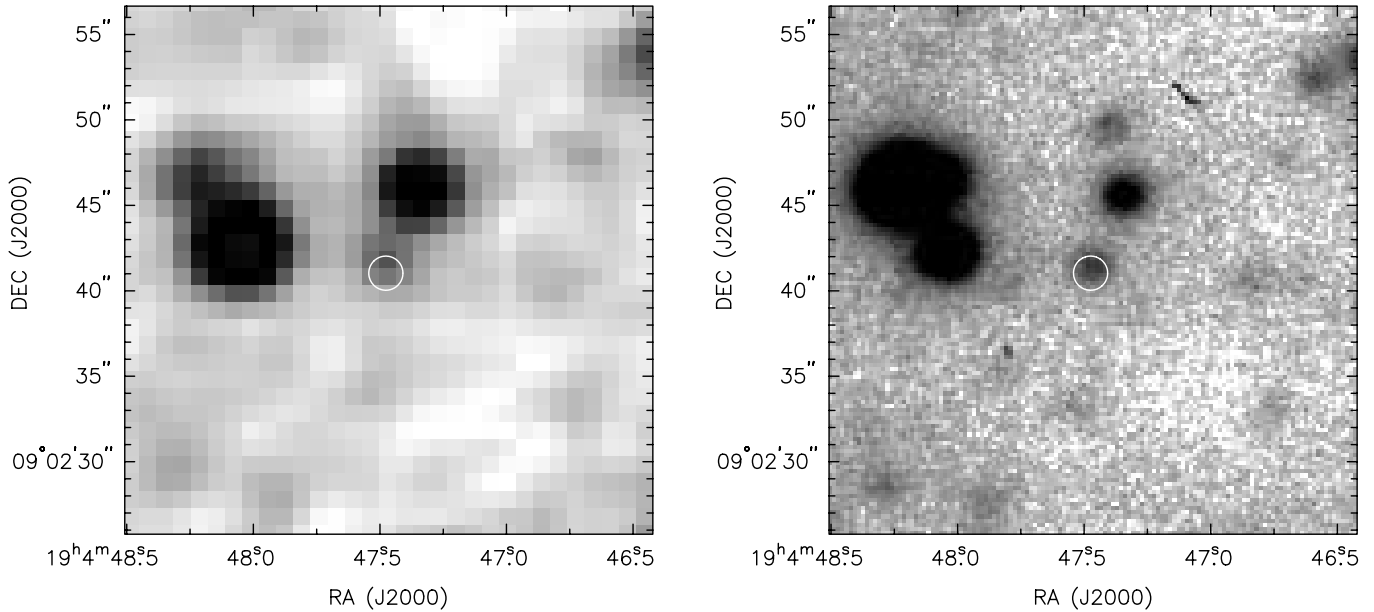


FIG. 5.—The *J*-band (left) and *R*-band (right) images of XTE J1906+090. Circles on each plot show the 1'' *Chandra* X-ray error regions (99.9% confidence level).

from XTE J1906+090, or if it was related to incomplete removal of SGR 1900+14 minibursts or to flux variations of other sources in the field.

2.3. Spectral Analysis

We generated the source spectrum using the same events as in the timing analysis. The background spectrum was extracted from a 2' circular region located in a source-free environment on the same ACIS-I chip. We grouped the time-integrated X-ray spectrum of the pulsar so that each spectral bin contained at least 25 counts.

We modeled the X-ray spectrum using XSPEC (ver. 11.3.2; Arnaud 1996) between 0.5 and 8.0 keV with a set of continuum models: power-law, blackbody, and thermal bremsstrahlung, all attenuated by interstellar absorption assuming the Wisconsin photoelectric cross sections and cosmic abundances (Morrison & McCammon 1983; XSPEC model *wabs*). Both the blackbody and power-law models provided a statistically acceptable fit to the data ($\chi^2/\nu = 27.2/33$ and $24.9/33$, respectively). The power-law fit to the phase-averaged spectrum resulted in an interstellar hydrogen column density of $n_{\text{H}} = 3.1^{+0.6}_{-0.5} \times 10^{22} \text{ cm}^{-2}$, a power-law index⁹ of $\Gamma = 1.3^{+0.3}_{-0.3}$, and an unabsorbed 2–10 keV flux¹⁰ of $F_{\text{X}} = 3.1^{+0.5}_{-2.0} \times 10^{-12} \text{ ergs cm}^{-2} \text{ s}^{-1}$. The blackbody fit resulted in $n_{\text{H}} = 1.6^{+0.4}_{-0.3} \times 10^{22} \text{ cm}^{-2}$, blackbody temperature $kT_{\text{BB}} = 1.5^{+0.2}_{-0.1} \text{ keV}$, and an unabsorbed flux of $F_{\text{X}} = 2.3^{+0.1}_{-0.4} \times 10^{-12} \text{ ergs cm}^{-2} \text{ s}^{-1}$. The thermal bremsstrahlung fit yields an unrealistically large plasma temperature ($kT_{\text{TB}} = 72 \pm 97 \text{ keV}$), and the large errors make this result even less meaningful. However, we obtain a lower limit plasma temperature of $\sim 12 \text{ keV}$ by using a fixed interstellar absorption of $n_{\text{H}} = 3.1 \times 10^{22} \text{ cm}^{-2}$ and stepping through fixed kT_{TB} values. Note that the Galactic n_{H} toward this source is $1.3 \times 10^{22} \text{ cm}^{-2}$ (Dickey & Lockman 1990).

Wilson et al. (2002) found an emission iron line in the X-ray spectrum of XTE J1906+090 during the 1998 outburst. We do

not detect any evidence of a line in the *Chandra* data; interestingly, no iron line was reported during the 1996 outburst (Marsden et al. 1998). Furthermore, to search for variation in the emitted spectrum as a function of spin phase, we have generated four spectra corresponding to four phase intervals with roughly equal numbers of source counts. We do not find any evidence for variation of the spectral parameters with the spin phase of XTE J1906+090.

2.4. Search for Source Activity in Archival RXTE Data

The 2–10 keV flux of XTE J1906+090 during the *Chandra* observation is $3 \times 10^{-12} \text{ ergs cm}^{-2} \text{ s}^{-1}$, roughly of the same order as the peak flux of its 1996 outburst, indicating that the source was very likely undergoing another epoch of activity in late 2003 May. To search for possible transient activity (pulsations) of XTE J1906+090 around the times of the *Chandra* pointing, we have investigated our SGR 1900+14 monitoring observations with the *RXTE* PCA¹¹ on 2003 June 2. We searched for pulsations from XTE J1906+090 by applying the Z^2_2 statistic on the energy-selected (1–20 keV) and barycenter-corrected PCA data. We do not detect any pulsations (3σ upper limit for pulsed flux is $3.8 \times 10^{-12} \text{ ergs cm}^{-2} \text{ s}^{-1}$) or any X-ray activity associated with XTE J1906+090 at the time of the *RXTE* PCA pointing, indicating that during the *Chandra* observations we may have detected a small portion of a weak outburst, lasting only for a few days.

3. OPTICAL OBSERVATIONS

The field of XTE J1906+090 was observed on 2004 July 16 with the 1.5 m RTT150 located at the TÜBİTAK National Observatory, Antalya, Turkey. An ANDOR DW436 CCD (2048 × 2048 pixels and $0''.24 \text{ pixel}^{-1}$) was used as the focal plane instrument. We performed the optical observations in $3' \times 3'$ CCD subarray mode and acquired 10 180 s exposures using the Cousins *R* filter. The seeing was around $1''.5$ throughout the

⁹ Error of the spectral parameter values are at the 90% confidence level.

¹⁰ The flux errors are computed via 1000 realizations in XSPEC.

¹¹ XTE J1906+090 lies within the field of view of the PCA during most SGR 1900+14 observations.

TABLE 2
2MASS OR USNO-B1.0 POINT SOURCES COINCIDENT WITH THE *Chandra* X-RAY SOURCES

| SOURCE NUMBER | 2MASS SOURCES | | | | USNO-B1.0 SOURCES | | | |
|---------------|------------------|-------------|-------------|-----------------|-------------------|-------------|-------------|-----------------|
| | Catalog Name | R.A. | Decl. | Offset (arcsec) | Catalog Name | R.A. | Decl. | Offset (arcsec) |
| 8..... | 19044747+0902419 | 19 04 47.47 | +09 02 41.9 | 0.31 | | | | |
| 5..... | 19054012+0904010 | 19 05 40.13 | +09 04 01.1 | 0.17 | 0990-0424597 | 19 05 40.13 | +09 04 01.0 | 0.22 |
| 9..... | 19045537+0859542 | 19 04 55.38 | +08 59 54.3 | 0.65 | 0989-0420922 | 19 04 55.39 | +08 59 53.9 | 0.27 |

NOTE.—Units of right ascension are hours, minutes, and seconds, and units of declination are degrees, arcminutes, and arcseconds.

observing run. We used appropriate IRAF NOAO (ver. 2.12.2) tasks to calibrate and reduce the images.

We have aligned and combined all 10 *R*-band images of the field of XTE J1906+090 to improve the S/N of our astrometry and photometry. We performed astrometry using the USNO-B1.0 catalog (Monet et al. 2003). Our best estimate for the position of the optical source is R.A. = $19^{\text{h}}04^{\text{m}}47^{\text{s}}.48$, decl. = $+09^{\circ}02'41''.8$, with an uncertainty of $0''.3$ at the 90% confidence level. In Figure 5 (*right*) we show the optical counterpart of XTE J1906+090 with the *Chandra* error circle. We also performed optical photometry on the combined *R*-band image. The photometric calibration was derived using stars in our field and in the USNO-B1 catalog. The resulting *R* magnitude of the source is 18.7 ± 0.1 .

3.1. 2MASS Detection of XTE J1906+090

We searched the Two Micron All Sky Survey (2MASS) database for an IR counterpart to XTE J1906+090. We found a point source at R.A. = $19^{\text{h}}04^{\text{m}}47^{\text{s}}.47$, decl. = $+09^{\circ}02'41''.9$ that is coincident with both the *Chandra* and the optical positions. (The 2MASS *J* image of the point source is shown in the left panel of Fig. 5.) We estimate the probability of having a point source with *J* magnitude brighter than 18 in 2MASS by chance coincidence within the *Chandra* error circle of XTE J1906+090 as 7.5×10^{-3} . Therefore, we conclude that the point source in 2MASS is the IR counterpart of XTE J1906+090 system. The 2MASS source has IR magnitudes of $J = 15.18 \pm 0.07$, $H = 14.17 \pm 0.11$, and $K = 13.50 \pm 0.06$. Table 2 lists the IR (2MASS) or/and optical (USNO-B1.0) point sources that are positionally coincident with XTE J1906+090 and the other X-ray sources we detected in the ACIS-I field.

4. DISCUSSION

4.1. XTE J1906+090 as a Transient Be/X-Ray Binary

XTE J1906+090 has undergone three outbursts to date, in 1996, 1998, and possibly in 2003, with (2–10 keV) luminosities of 7×10^{34} , 7×10^{36} , and 4×10^{34} ergs s^{-1} , respectively, for an assumed distance of 10 kpc (Marsden et al. 1998). The observed outbursts appear isolated and not part of a series evenly spaced at the orbital period; they vary considerably in peak intensity, and two of the three are at least an order of magnitude fainter than typical normal outbursts. However, these effects are more closely related to the sensitivity of the observing instruments than to intrinsic source behavior. The average frequency rate was $(-5.7 \pm 0.1) \times 10^{-14}$ Hz s^{-1} between the 1996 and 1998 outbursts, while between 1998 and 2003 the average frequency rate increased by a factor of about 7 to $(-3.96 \pm 0.03) \times 10^{-13}$ Hz s^{-1} .

XTE J1906+090 resembles several confirmed Be/X-ray binaries, e.g., Cepheus X-4 (Wilson et al. 1999), 4U 1145–619

(Wilson-Hodge 1999), SAX J2103.5+4545 (Baykal et al. 2002), and X Per (Delgado-Martí et al. 2001). Like XTE J1906+090, the 66 s pulsar Cep X-4 has undergone three known outbursts (in 1988, 1993, and 1997) that appeared to be isolated normal outbursts. Between outbursts, the pulsar was spinning down, and the spin-down rate between the 1997 and 1993 outbursts was a factor of about 10 larger than that between the 1988 and 1993 outbursts. During the 1997 outburst, the measured frequency rate was $\sim -10^{-12}$ Hz s^{-1} , approximately the same as that measured in the 1998 outburst of XTE J1906+090 and likely due to orbital motion in both systems. Unlike XTE J1906+090, Cep X-4's outbursts had more typical luminosities of $\sim 10^{36}$ ergs s^{-1} . The peak outburst fluxes of the 297 s pulsar 4U 1145–619 are highly variable, like XTE J1906+090's, varying by a factor of about 15. This source is much brighter than XTE J1906+090; however, like XTE J1906+090, all of its outbursts appear to be normal outbursts, and it shows a global spin-down trend. The source 4U 1145–619 is unusual because rather than showing clearly defined giant and normal outbursts, it has outbursts covering the full range of intensities from typical normal to typical giant outbursts, but all of the outbursts are similar in duration, show no large spin-up episodes, and are evenly spaced at the presumed orbital period (Wilson-Hodge 1999). Finally, the 358 s X-ray pulsar SAX J2103.5+4545, which has the shortest known orbital period (12.7 days) for a confirmed Be/X-ray binary (Reig et al. 2004), underwent an extended period of activity, about 200 days in 1999 and 2000, during which it exhibited a 100 day spin-up episode (Baykal et al. 2002). SAX J2103.5+4545's outburst resembled a giant outburst, but like the 1998 outburst from XTE J1906+090, its luminosity was low, about 10^{35} – 10^{36} ergs s^{-1} over the course of the outburst.

4.2. On the 2MASS Infrared Counterpart of XTE J1906+090

Zhang et al. (2005) recently compiled a catalog of 1136 relatively bright, isolated Be stars ($J < 10.8$) detected in the 2MASS mission. They provide a plot of the dereddened ($J - H$) color versus the ($H - K$) color of all these systems (Fig. 1 in Zhang et al. 2005). According to their estimates, the bulk majority of bright Be stars have dereddened ($J - H$) colors between -0.20 and 0.10 , and dereddened ($H - K$) colors between -0.15 and 0.25 . Zhang et al. (2005) estimated the visual extinction (A_V) values using the color excess $[E(B - V)]$ term and the standard extinction law (Rieke & Lebofsky 1985).

To determine where our proposed IR counterpart to XTE J1906+090 falls within the color-color trend of 2MASS Be stars (Zhang et al. 2005) and to compare the IR color characteristics of the source with those of confirmed Be/X-ray binary systems, we have calculated its dereddened IR magnitudes as follows. We estimated the visual extinction, A_V , as 14.3 using the column density $n_{\text{H}} = 3.1 \times 10^{22}$ cm^{-2} and the approximate conversion relationship given by Weingartner & Draine (2001). We then computed the extinction coefficients in *J*, *H*, and *K* bands using

the method given by Cardelli et al. (1989). The dereddened IR colors of the 2MASS source were calculated as $(J - H)_d = -0.50$ and $(H - K)_d = -0.58$. Based on these estimates, the IR emission of XTE J1906+090 appears to be more reddened compared to the bright Be stars. However, the dereddened IR colors of a recently confirmed Be/X-ray system, GRO J2058+42 (Wilson et al. 2005), are $(J - H)_d = -0.56$ and $(H - K)_d = -0.50$, very similar to the ones we determined for the IR counterpart of XTE J1906+090. On the other hand, if we use $n_H = 1.6 \times 10^{22} \text{ cm}^{-2}$, we obtain the dereddened IR colors of XTE J1906+090 as $(J - H)_d = 0.22$ and $(H - K)_d = 0.06$, which are well within the colors of the bulk majority of Be stars.

4.3. Implications of the Centrifugal Inhibition Regime for XTE J1906+090

Since pulsations were detected from XTE J1906+090 with *Chandra*, the source was likely not in the centrifugal inhibition of accretion regime (Stella et al. 1986). By comparing the estimated luminosity at the onset of this regime to our measured flux with *Chandra*, we can derive a constraint on the distance. Centrifugal inhibition of accretion occurs when the magnetospheric radius (Pringle & Rees 1972; Lamb et al. 1973), which defines the region in which motion of material is determined by the magnetic field, is outside the corotation radius. Wilson et al. (2003) derived the flux at the onset of centrifugal inhibition of accretion. Here we have substituted XTE J1906+090's period into their equation (17),

$$F_X^{\min} \simeq 5 \times 10^{-11} \text{ ergs cm}^{-2} \text{ s}^{-1} k^{7/2} \mu_{30}^2 M_{1.4}^{-2/3} R_6^{-1} P_{89.66}^{-7/3} d_{\text{kpc}}^{-2}, \quad (1)$$

where μ_{30} , $M_{1.4}$, R_6 , and $P_{89.66}$ are the pulsar's magnetic moment in units of 10^{30} G cm^3 , mass in units of $1.4 M_\odot$, radius in units of 10^6 cm , and spin period in units of 89.66 s, respectively; d_{kpc} is the distance in kiloparsecs, and k is a constant factor of order 1. For the *Chandra* observation, we measured $F = 3.1 \times 10^{-12} \text{ ergs cm}^{-2} \text{ s}^{-1}$. Since pulsations were detected, we assume $F \gtrsim F_X^{\min}$ and solve for d_{kpc} in terms of μ_{30} ,

$$d_{\text{kpc}} \gtrsim 4.0 k^{7/4} \mu_{30}. \quad (2)$$

The *Chandra* observation of XTE J1906+090 was not scheduled to catch an outburst; hence, there are two potential explanations for the observed emission: either we are seeing reasonably frequent but often undetectable normal outbursts, or we are observing quiescent emission. The quiescent emission may result from variable emission due to leakage or magnetospheric accretion if the pulsar is in the propeller (centrifugal inhibition) regime. A normal transient outburst, such as that observed in 1998, would occur when the incoming mass flow reaches the centrifugal threshold. Within this picture, the low-frequency variability seen with *Chandra* could result from the unstable accretion expected near the accretion/propeller transition. More observations with sensitive instruments such as *Chandra* and *XMM-Newton* are needed in order to understand the low-luminosity behavior of Be/X-ray transients.

5. CONCLUSIONS

We have identified and precisely localized XTE J1906+090 using archival *Chandra* observations. In light of this identification, we discovered the optical and infrared counterparts of the system. We conclude that the source was in outburst during 2003. Based on the fluxes of three identified outbursts of the system, we suggest that XTE J1906+090 displays a wider variety of outbursts than normal or giant outbursts. Moreover, we were able to place a distance lower limit of 4 kpc for an assumed magnetic moment of the neutron star. Finally, we argue that XTE J1906+090 shows numerous similarities with the confirmed Be/X-ray binary systems. However, the absolute confirmation of the Be star nature of the companion can only be deduced by observing Balmer emission lines in the optical spectrum of the system, which are now possible with the herein identified source counterpart.

E. G. acknowledges partial support by the Turkish Academy of Sciences through grant E. G/TUBA-GEBIP/2004-11. S. K. P. and P. M. W. acknowledge the support from NASA through grant NAG 5-13739. We thank the anonymous referee for valuable suggestions.

REFERENCES

- Arnaud, K. A. 1996, in ASP Conf. Ser. 101, *Astronomical Data Analysis Software and Systems V*, ed. G. Jacoby & J. Barnes (San Francisco: ASP), 17
- Baykal, A., Stark, M. J., & Swank, J. H. 2002, *ApJ*, 569, 903
- Buccheri, R., et al. 1983, *A&A*, 128, 245
- Cardelli, J. A., Clayton, G. C., & Mathis, J. S. 1989, *ApJ*, 345, 245
- Coe, M. J. 2000, in ASP Conf. Ser. 214, *Be Phenomenon in Early-Type Stars*, ed. M. A. Smith & H. F. Henrichs (San Francisco: ASP), 656
- Delgado-Martí, H., Levine, A. M., Pfahl, E., & Rappaport, S. A. 2001, *ApJ*, 546, 455
- Dickey, J. M., & Lockman, F. J. 1990, *ARA&A*, 28, 215
- Garmire, G. P., Bautz, M. W., Ford, P. G., Nousek, J. A., & Ricker, G. R. 2003, *Proc. SPIE*, 4851, 28
- Lamb, F. K., Pethick, C. J., & Pines, D. 1973, *ApJ*, 184, 271
- Marsden, D., Gruber, D. E., Heindl, W. A., Pelling, M. R., & Rothschild, R. E. 1998, *ApJ*, 502, L129
- Monet, D. G., et al. 2003, *AJ*, 125, 984
- Morrison, R., & McCammon, D. 1983, *ApJ*, 270, 119
- Negueruela, I. 1998, *A&A*, 338, 505
- Porter, J. M., & Rivinius, T. 2003, *PASP*, 115, 1153
- Pringle, J. E., & Rees, M. J. 1972, *A&A*, 21, 1
- Reig, P., Negueruela, I., Fabregat, J., Chato, R., Blay, P., & Mavromatakis, F. 2004, *A&A*, 421, 673
- Rieke, G. H., & Lebofsky, M. J. 1985, *ApJ*, 288, 618
- Stella, L., White, N. E., & Rosner, R. 1986, *ApJ*, 308, 669
- Swartz, D. A., Ghosh, K. K., McCollough, M. L., Pannuti, T. G., Tennant, A. F., & Wu, K. 2003, *ApJS*, 144, 213
- Takeshima, T., & Murakami, T. 1998, *IAU Circ.*, 7032, 2
- Weingartner, J. C., & Draine, B. T. 2001, *ApJ*, 548, 296
- Weisskopf, M. 2004, *Proc. SPIE*, 5488, 25
- Wilson, C. A., Finger, M. H., Coe, M. J., & Negueruela, I. 2003, *ApJ*, 584, 996
- Wilson, C. A., Finger, M. H., Göğüş, E., Woods, P., & Kouveliotou, C. 2002, *ApJ*, 565, 1150
- Wilson, C. A., Finger, M. H., & Scott, D. M. 1999, *ApJ*, 511, 367
- Wilson, C. A., Weisskopf, M. C., Finger, M. H., Coe, M. J., Grenier, J., Reig, P., & Papamastorakis, G. 2005, *ApJ*, 622, 1024
- Wilson-Hodge, C. A. 1999, Ph.D. thesis, Univ. Alabama, Huntsville
- Zhang, P., Chen, P. S., & Yang, H. T. 2005, *NewA*, 10, 325

ERRATUM: “*CHANDRA* LOCALIZATION OF XTE J1906+090 AND DISCOVERY OF ITS OPTICAL AND INFRARED COUNTERPARTS” (ApJ, 632, 1069 [2005])

ERSIN GÖĞÜŞ,^{1,2} SANDEEP K. PATEL,^{2,3} COLLEEN A. WILSON,^{3,4} PETER M. WOODS,^{2,3} MARK H. FINGER,^{2,3} AND CHRYSsa KOUVELIOTOU^{3,4}

Because of an error at the Press, the listings for affiliations 1 and 2 were incorrect. The correct affiliations are:

¹Sabancı University, Faculty of Engineering and Natural Sciences, Orhanlı–Tuzla, İstanbul, Turkey; ersing@sabanciuniv.edu.

²Universities Space Research Association, NSSTC, 320 Sparkman Drive, Huntsville, AL 35805.

³XD-12, Space Science Branch, National Space Science and Technology Center, 320 Sparkman Drive, Huntsville, AL 35805.

⁴NASA Marshall Space Flight Center.

The Press sincerely regrets this error.